# Range and energetics of charge hopping in organic semiconductors

Hassan Abdalla, Guangzheng Zuo, and Martijn Kemerink[*]

*Complex Materials and Devices, Department of Physics, Chemistry and Biology (IFM), Linköping University, SE-581 83 Linköping, Sweden*

(Received 21 September 2017; revised manuscript received 1 November 2017; published 22 December 2017)

The recent upswing in attention for the thermoelectric properties of organic semiconductors (OSCs) adds urgency to the need for a quantitative description of the range and energetics of hopping transport in organic semiconductors under relevant circumstances, i.e., around room temperature (RT). In particular, the degree to which hops beyond the nearest neighbor must be accounted for at RT is still largely unknown. Here, measurements of charge and energy transport in doped OSCs are combined with analytical modeling to reach the univocal conclusion that variable-range hopping is the proper description in a large class of disordered OSC at RT. To obtain quantitative agreement with experiment, one needs to account for the modification of the density of states by ionized dopants. These Coulomb interactions give rise to a deep tail of trap states that is independent of the material's initial energetic disorder. Insertion of this effect into a classical Mott-type variable-range hopping model allows one to give a quantitative description of temperature-dependent conductivity and thermopower measurements on a wide range of disordered OSCs. In particular, the model explains the commonly observed quasiuniversal power-law relation between the Seebeck coefficient and the conductivity.

The recent boom in attention for organic thermoelectrics has led to very encouraging practical results, but a predictive formal framework appears lacking [1,2]. In particular, the observation of a power-law relation between the Seebeck coefficient and the conductivity of *p*-type organic (semi)conductors has puzzled the community [3,4]. Recently, Kang and Snyder derived an empirical model that accurately reproduces this observation, but as their model lacks a transparent connection to a charge transport mechanism, it offers limited fundamental insight [5].

Charge transport in disordered organic semiconductors (OSCs) is commonly assumed to occur via phonon-assisted tunneling (hopping) between localized sites. Even when considering relatively simple implementations of hopping models, using, e.g., Miller-Abrahams or Marcus rates and a static, typically Gaussian or exponential distribution of site energies, there are fundamentally different approaches that can be hard to distinguish experimentally [6]. On the one hand, lattice models with parameters that give rise to nearest-neighbor hopping (NNH) have been successful in rationalizing the temperature and concentration dependence of the charge-carrier mobility in OSCs around room temperature [7,8]. On the other hand, Mott's variable-ange hopping (VRH) theory has been the basis of VRH models describing the very same phenomena [9,10]. Technically speaking, nearest-neighbor lattice models give rise to a temperature-independent transport energy [8], whereas VRH models yield a temperature-dependent transport energy [10]—the transport, or critical energy, is the upper energy in the characteristic hop in the percolating network. Although NNH is a limit of VRH and transitions between NNH and VRH as a function of temperature or site density can occur [10], the degree to which non-nearest-neighbor hops are relevant to the description of charge motion in "typical" OSCs under practical conditions (room temperature) has not been answered. The foremost reason for this is the inconclusiveness of typical experimental charge transport investigations which is illustrated in Fig. 1(a) where conductivity vs doping concentration curves have been calculated from NNH and VRH using Miller-Abraham rates. Especially at lower carrier concentrations, there is little difference between the two hopping mechanisms, apart from a scaling factor. The same indistinctness is found for free charge carriers, i.e., in absence of doping, as shown in Sec. 3 of the Supplemental Material (SM) [11].

In more recent work, using multiscale modeling techniques and including, e.g., the effects of polarization and dynamic and/or static transfer integral disorder, significant advances over simple Mott- and Bässler-type models discussed above have been made [12–15]. In particular, *ab initio* calculations by Massé *et al.* showed that long-range (non-nearest-neighbor) hops can be enabled by a superexchange mechanism and can contribute strongly to the field dependence of the mobility; at the same time, the low-field conductivity was only slightly increased by these hops [16]. These approaches are computationally very demanding and so far do not address thermoelectric properties, which makes them rather unsuited for our current purposes: to develop a transparent physical model that can describe experimental observations of charge and energy transport in a wide range of doped organic semiconductors and to assess to which degree hops beyond the nearest neighbor are relevant under practical conditions.

Here, we show that by confronting combined conductivity and thermopower measurements with analytical modeling, NNH and VRH can be well distinguished. In particular, we find that classical Mott-type VRH in a Gaussian density of states (DOS) modified by Coulomb trapping of ionized dopants leads to a consistent description of charge and energy transport in doped OSCs around RT, as evidenced by the reproduction of the quasiuniversal power-law relationship between the Seebeck coefficient and conductivity [3,4]. This conclusion is further substantiated by the favorable comparison of analytically and experimentally obtained temperature dependences of both the conductivity and the thermopower.
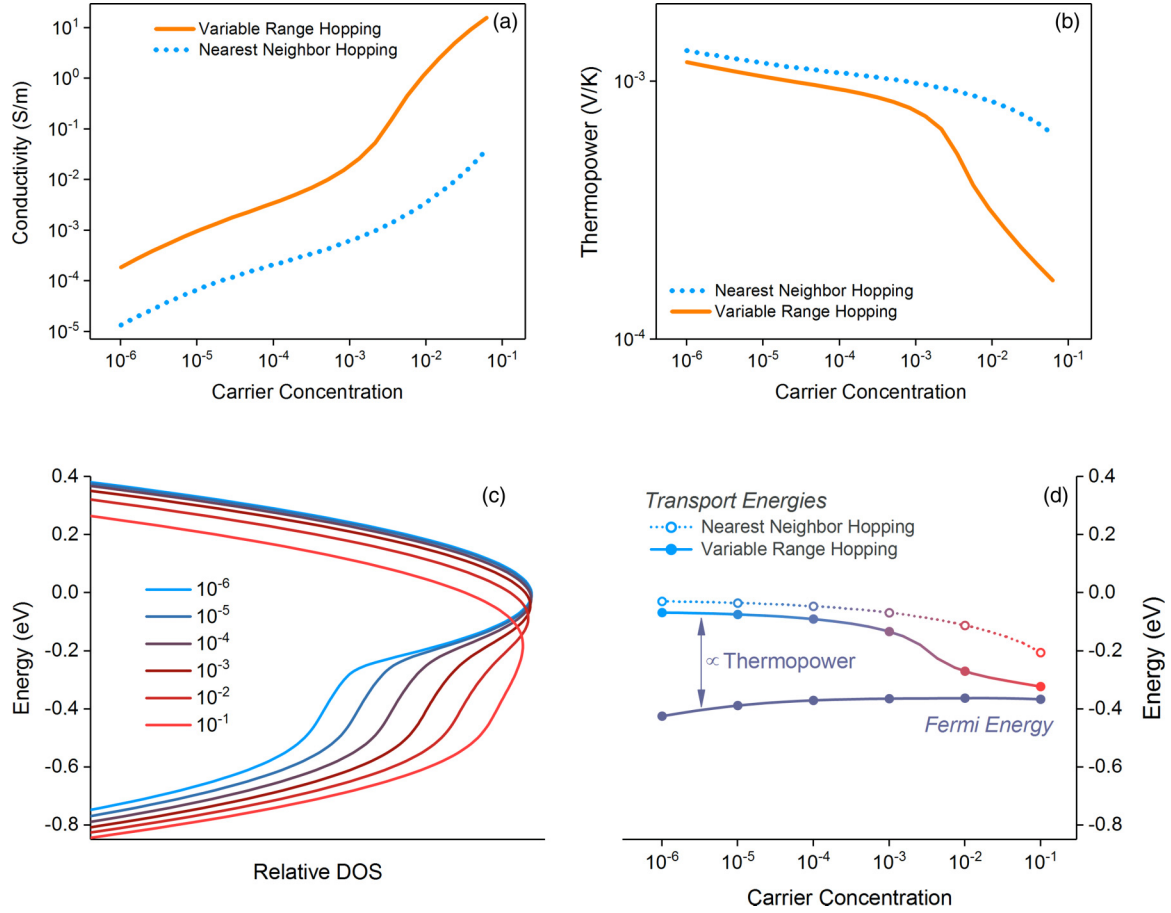
_____

*Corresponding author: martijn.kemerink@liu.se

FIG. 1. Discerning variable-range hopping from nearest-neighbor hopping. Calculated dopant-induced carrier concentration depedence of (a) conductivity and (b) thermopower. (c) DOS calculated from the analytical model parametric in charge-carrier concentration. (d) Fermi energy $E_F$ and transport energy $E^*$ with respect to the DOS in panel (c), calculated for VRH and NNH leading to the carrier concentration dependence of conductivity (a) and thermopower (b). Carrier concentrations are relative to the total DOS. Model parameters are given in Table S1 of the SM [11].

In Fig. 1 and the following we use a recently developed model to calculate both the conductivity and the thermopower versus dopant-induced charge-carrier concentration. In Refs. [17,18] the model has been benchmarked against kinetic Monte Carlo simulations and shown to accurately reproduce the measured conductivity of both intrinsic and doped OSCs over a wide concentration range, with minor deviations occurring at molar doping concentrations approaching 10%. For comparison with kinetic Monte Carlo simulations NNH was previously assumed, but the model can easily be modified to capture either NNH or VRH. In either case, it is assumed that the conductivity $\sigma$ is dominated by a characteristic hop between the Fermi energy $E_F$ and some critical energy $E^*$ that reflects the characteristic hop in the percolating network [8,10]. Evidently, $E_F$ does not depend on the choice of hopping model, whereas $E^*$ does, as illustrated in Fig. 1(d). The key ingredient of the model is that the DOS, with respect to which the characteristic energies $E_F$ and $E^*$ are calculated, varies with doping concentration as shown in Fig. 1(c). An exponential tail of deep states develops in the intrinsically Gaussian DOS due to the attractive Coulomb potential of ionized dopants [19,20]. Further details about the model can be found in SM Sec. 2 where we also justify the implicit

assumption that the material is homogeneous. Note also that similar DOS tails as calculated here have been experimentally observed by ultraviolet photoemission spectroscopy [11,21].

The rationalization of our method to distinguish NNH and VRH is the fact that the experimentally accessible Seebeck coefficient is a direct measure of the energy difference $\Delta E = E^* - E_F$ and can therefore be used to test the significantly different predictions for the critical energy $E^*$ by both models that are shown in Fig. 1(d). As explained above, the common assumption in percolation models, including ours, is that the conductivity is proportional to a simple Arrhenius factor as $\sigma \propto \exp(-\Delta E / k_B T)$—note, though, that $\Delta E$ is typically temperature dependent [22]. Along the same line, the energy that a charge takes along upon moving, i.e., the Peltier coefficient, is then in lowest-order approximation $\Pi = \Delta E$. Using Onsager's reciprocity relation, this leads to a Seebeck coefficient that is given by $S = \Pi / T = (E^* - E_F)/T$. Figure 1(b) shows that indeed NNH and VRH models lead to substantially different predictions for $S$ at carrier concentrations above $10^{-3}$.

The physical reason for the different behaviors of $S$ in NNH and VRH models is the following. In VRH any change in temperature or, as is the case here, DOS shape, leads to a change in both the typical (spatial) hopping distance $R^*$ and

the critical energy $E^*$ that are connected through the demand that a percolating path can be formed for the given combination of $R^*$ and $E^*$. The possibility to search for an optimal, i.e., giving the highest conductivity, combination of $R^*$ and $E^*$ does not exist in NNH, as $R^*$ is constant and equal to the nearest-neighbor distance. Hence, a weaker dependence of $E^*$ on temperature and doping concentration, i.e., DOS shape, may be expected. This is further outlined in SM Sec. S7 [11]. In fact, Cottaar *et al.* have shown that for a Gaussian DOS in this case $E^*$ is a constant that only depends (linearly) on the width of the DOS [8]. This dependency was found to hold for both Miller-Abrahams and Marcus hopping rates, albeit with different prefactors. Zuo *et al.* have shown that adhering to an $E^*$ that sits a fixed distance below the DOS maximum gives an accurate description of the conductivity even in the case that dopant ions give rise to an exponential tail in the DOS [17]. Hence, the modest shift in $E^*$ for NNH in Fig. 1(d) solely reflects the minor downward shift of the DOS maximum, whereas the much larger shift for VRH is caused by the increasing number of accessible states in the direct vicinity of the Fermi level.

To connect these considerations to reality, we conducted a transport and thermopower investigation of thin films of common polymers poly(3-hexylthiophene-2,5-diyl) (P3HT), poly[2,6-(4,4-bis-(2-ethylhexyl)-4H-cyclopenta[2,1-b;3,4-b′]-dithiophene)-alt-4,7-(2,1,3-benzothiadiazole)] (PCPDTB-T), poly[4,8-bis[(2-ethylhexyl)-oxy]benzo[1,2-b:4,5-b]dithiophene-2,6-diyl][3-fluoro-2-[(2-ethylhexyl)carbonyl]thieno[3,4-b]thiophenediyl] (PTB7), poly(2-methoxy, 5-(2′ ethylhexyloxy)-p-phenylene vinylene) (MEH-PPV), doped with 2,3,5,6-tetrafluoro-7,7,8,8-tetracyanoquinodimethane ($F_4TCNQ$) in relative molar concentrations ranging from $10^{-4}$ to $10^{-1}$. To further stress the general nature of our results, experiments were also conducted on P3HT:PTB7 blend films as well as PPV:PS blends doped by iodine vapor; as these lead to similar results as for single polymer films, they will not be discussed separately. Molecular doping was done in two different ways, bulk and surface doping [23], to ensure that the results are also independent of the doping method used. In addition, this allowed one to cover a wider conductivity range. Bulk doping was achieved by blending $F_4TCNQ$ and the polymer in solution before spin coating the resulting solution onto a glass substrate. Surface doping was achieved by spin coating a layer of $F_4TCNQ$ on top of a previously spin-coated polymer layer. Further details on device preparation, characterization techniques, and full compound names can be found in SM Sec. 1 [11].

In order to circumvent the well-known problem of having no exact control over the actual free-charge-carrier density, we followed the example of Glaudell *et al.* and plotted the conductivity dependence of the thermopower for all samples as solid gray circles in Fig. 2 [3]. The result stands in good agreement with previously published experimental results, as shown by the shaded green symbols. The experimental data also follows the "universal" $-1/4$ power-law relationship (gray solid line) that was previously noted by Glaudell *et al.* We combined the analytically obtained conductivity and thermopower data from Figs. 1(a) and 1(b), to obtain the full (VRH) and dotted (NNH) lines in Fig. 2. Although NNH does lead to power-law-like behavior, its exponent is significantly
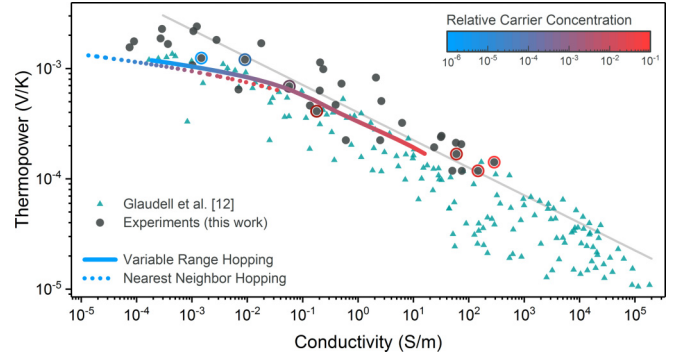


FIG. 2. Thermopower vs conductivity of doped disordered organic semiconductors. Gray full circles are experiments, green triangles are multisource experimental data as assembled in Ref. [3], and colored lines are calculated with the analytical model parametric in carrier concentration (relative to the total DOS) as indicated in the legend. The VRH model clearly reproduces the $-1/4$ power-law relationship observed experimentally (gray line). The colored rings highlight the subset of the experimental data that has been used in the investigation of the temperature dependence in Fig. 3. Model parameters are given in Table S1 of the SM [11].

less than experimentally observed. Importantly, the functional shape and the exponent are essentially independent of the five input parameters of the model, most notably the width of the initially Gaussian DOS $\sigma_{DOS}$, as shown in detail in SM Sec. 4 [11]. The important consequence of this is that it is impossible to reproduce the approximate power-law slope of $-1/4$ with the nearest-neighbor hopping model. In passing we note that the same holds for trap-and-release models that employ a constant mobility edge as these have the same mathematical structure as our NNH model [24].

Variable-range hopping, on the other hand, produces a kinked shape of the conductivity dependence that reproduces the experimentally observed $-1/4$ power law at high conductivities, while flattening out at lower conductivities. Upon close inspection this can also be observed in our experiments. The leveling off at low conductivity was noted before in the work by Kang and Snyder [5]. In that work, the observation of a "kinked power law" in a large group of doped OSCs was interpreted in terms of a phenomenological transport function. Even though the shape of the resulting $S$ vs $\sigma$ curves is virtually identical to the present result, the power-law shape of the transport function used in Ref. [5] is incompatible with any of the present hopping models (see Sec. 2 of the SM [11]). Exploration of the parameter space of the VRH model in SMI Sec. 4 shows that the kinked power-law shape, with an exponent around $-1/4$, is a rather robust feature of the model [11]. At the same time, parameter variation does allow one to fit essentially any subset of data in Fig. 2. As this is not the purpose of this work, this shall not be pursued further. In addition, the interchangeability of some of the parameters in the model, e.g., in the inverse localization radius $\alpha$ and the attempt to hop frequency $\nu_0$, makes it hard to determine parameters with great accuracy. We therefore fixed $\alpha$ to $0.5 \times 10^9 \, \mathrm{m}^{-1}$ for all simulations shown in the main text. Interestingly, the resulting hopping range of several nanometers is similar to the typical intersite distances found in the work by Martens *et al.* where it is proposed
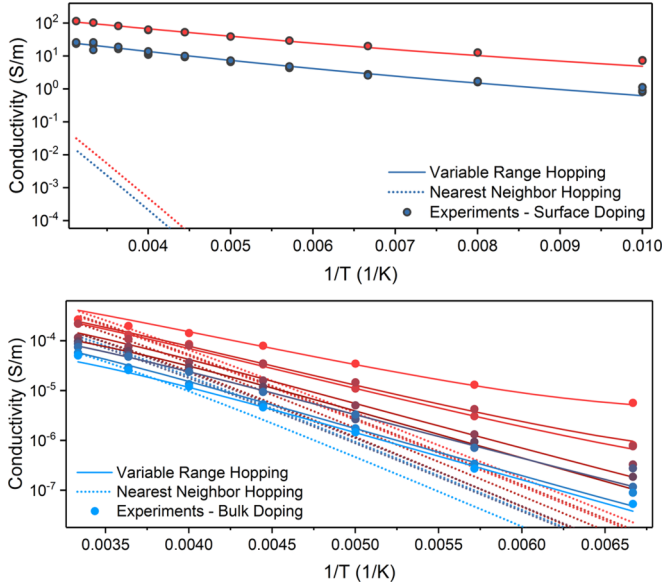
FIG. 3. Conductivity vs temperature parametric in doping concentration. Dashed and solid lines are calculated from the analytical NNH and VRH models, respectively, using the same parameters. The line colors indicate high (red) to low (blue) concentrations. Full circles are experimentally obtained from the ($F_4$TCNQ-doped P3HT) samples indicated in Fig. 2 by colored rings. The symbol colors indicate high (red) to low (blue) conductivities. For clarity, surface-doped (top figure) and bulk-doped (bottom figure) samples are plotted on different scales. Model parameters including color codes are given in SM Sec. 5 [11].

that charge-carrier delocalization increases with doping level [25]. Below, we will show that the present formalism does not require this assumption to be made.

As for the NNH model, the power-law slopes coming from the VRH model are largely independent of the parameter set used, rationalizing the quasiuniversal trend observed experimentally for a wide variety of OSC and doping methods. Within the current framework, the spread between materials can be quantitatively explained in terms of reasonable variations in the model's input parameters (see SM Sec. 4 [11]). Counterintuitively, up- or downward shifts of the $S$ vs $\sigma$ curve are largely impossible; particularly varying $\sigma_{DOS}$, the initial width of the DOS, has only a minor effect on the $-1/4$ power-law part of the curve, but rather extends it toward higher or lower conductivities. The reason being that in this regime both $E_F$ and $E^*$ are governed by the dopant-induced tail of the DOS (see Fig. 1). Importantly, the findings in Fig. 2 imply that already at room temperature substantial hopping beyond the nearest neighbor occurs.

To test our conclusion about charge motion in OSC occurring through a variable-range hopping process, we performed a detailed study of the temperature dependency of the conductivity. Figure 3 shows the conductivity of samples with the same doping concentrations as those marked by circles in Fig. 2 in the temperature range of 100 K (upper panel) or 150 K (lower) to 320 K together with model fits; the used fitting parameters and experimental details are given in SM Secs. 5 and 1, respectively [11]. Focusing on the model calculations first, it is clear that NNH and VRH predict very distinct trends

and curvatures for $\sigma(T)$. As was the case for the data in Fig. 2, it is impossible to mimic the behavior of one model by changing the parameters in the other. Clearly, the VRH model allows an excellent fit to our experiments, which is impossible with the NNH version of the model. A more detailed investigation of the functional shape of the $\sigma(T)$ curves using the concept of the reduced activation energy leads to the same conclusion that transport in these samples predominantly occurs through a VRH process, as shown in SM Sec. 6 [11]. In SM Sec. 8 we analyze two sets of literature data reporting combined $\sigma(T)$ and $S(T)$ curves, again only leading to a consistent description when using a VRH model [11].

In view of the low conductivity at lower temperatures for bulk-doped samples, the temperature-dependent data in the lower panel of Fig. 3 had to be measured on out-of-plane devices that do not allow simultaneous thermopower measurements. As a consequence, the magnitudes of the room-temperature conductivity are one to two orders of magnitude lower than those of the nominally identical active layers in Fig. 2 that were measured in-plane. Very similar anisotropy has been observed by Tanase *et al.* [26]. Importantly, the combined results in Figs. 2 and 3 show that despite the anisotropy, both in- and out-of-plane transport occur through a VRH mechanism.

The results above consistently show that charge and energy transport in our samples can consistently be described with a variable-range hopping model, but not with a nearest-neighbor hopping one. The same holds for a wide range of literature data as seen in Fig. 2 and detailed in SM Sec. 8 [11]. While giving rise to significant hopping beyond nearest neighbors, the fact that the typical localization radius $1/\alpha = 2$ nm we used to describe the data is about equal to the typical intersite distance $a_{NN}$ (1.8 nm) may appear to be at conflict with the assumption of incoherent hopping between localized states that underlies the transport model. First, Sec. S4 shows that changes by a factor 2 in (inverse) localization length do not affect agreement with experiment [Fig. S3(a)]. Significantly shorter localization lengths do, of course, suppress variable-range hopping and will reduce the agreement with experiment. Second, the relatively large value for $a_{NN}$ that was obtained from detailed analysis of transport experiments on single-carrier and solar cell devices [27–29] makes that estimated values of the corresponding transfer integrals remain well below values for which localization ceases to be important, as discussed in detail in SM Sec. 9 [11].

The final question to be addressed here is the range of materials for which this result can be expected to hold. First, all data in Figs. 2 and 3 have been obtained on doped samples so one could argue that the VRH hopping is somehow induced or facilitated by the dopants. However, especially Fig. 3 strongly suggests that even the lowest concentrations used ($10^{-4}$) require a description in terms of VRH. At such low dopant loadings it is unrealistic to assume transport to take place only through dopant-connected sites. Hence, we expect these results to hold for free charge carriers too, as encountered in, e.g., space-charge limited diodes or field effect transistors. Further, as indicated in the text, the mathematical structure of the NNH version of the model will not change upon changing from Miller-Abrahams- to Marcus-type hopping, and is in fact identical to trap-and-release type models with a fixed mobility edge. Hence, explicit evaluation of such variants will

not lead to any different conclusions than the current NNH model.

The model we used builds on the concept of significant static energetic disorder, which implies that highly ordered materials and especially single crystals fall outside the scope of our conclusions [30,31], as do materials showing metallic characteristics like an absolute thermopower that increases with temperature [32,33]. The same probably holds for many, if not all, members of the Poly(3,4-ethylenedioxythiophene) (PEDOT) family of materials for which a different functional shape than shown in Fig. 2 was demonstrated in the work of Kang and Snyder [5]. The reasons for this are unclear at present but may be associated with the complicated hierarchical morphology of PEDOT-type materials [34]. Nevertheless, as the empirical power law in Fig. 2 extends to high-conductivity materials that cannot be captured in the current model, one may speculate that even for these materials the VRH mechanism that leads to the characteristic slope of $-1/4$ is somehow relevant.

In conclusion, we have studied the charge and energy transport in disordered organic semiconductors, $p$-type doped from very low to very high concentrations. The experimental results have been analyzed using a simple analytical model, taking either variable-range hopping or nearest-neighbor hopping as basis, leading to the conclusion that only the former, variable-range hopping mechanism can consistently describe our data and trends observed in literature. Hence, in the class of doped, energetically disordered organic semiconductors we focus on, charge carriers do, at room temperature, to a significant degree hop to non-nearest-neighbor sites, and as such can adapt the hopping range to, e.g., changes in temperature or, in the case of doping, in the shape of the density of states. In particular, our results rationalize the occurrence of a quasiuniversal power-law relation between the Seebeck coefficient and the conductivity that is commonly observed in a broad class of materials—essentially those materials that are dominated by static energetic disorder. In this power-law regime, charge and energy transport are dominated by deep states that are induced by the dopant ions; the shape of this tail depends only weakly on material parameters like intrinsic disorder, leading to a nearly constant and universal (apparent) power-law slope of about $-1/4$.

[1] O. Bubnova, Z. U. Khan, A. Malti, S. Braun, M. Fahlman, M. Berggren, and X. Crispin, Nat. Mater. **10**, 429 (2011).

[2] K. Shi, F. Zhang, C.-A. Di, T.-W. Yan, Y. Zou, X. Zhou, D. Zhu, J.-Y. Wang, and J. Pei, J. Am. Chem. Soc. **137**, 6979 (2015).

[3] A. M. Glaudell, J. E. Cochran, S. N. Patel, and M. L. Chabinyc, Adv. Energy Mater. **5**, 1401072 (2015).

[4] A. B. Kaiser, Rep. Prog. Phys. **64**, 1 (2001).

[5] S. Dongmin Kang and G. Jeffrey Snyder, Nat. Mater **16**, 252 (2016).

[6] H. Bässler, Phys. Status Solidi B **175**, 15 (1993).

[7] W. F. Pasveer, J. Cottaar, C. Tanase, R. Coehoorn, P. A. Bobbert, P. W. M. Blom, D. M. de Leeuw, and M. A. J. Michels, Phys. Rev. Lett. **94**, 206601 (2005).

[8] J. Cottaar, L. J. A. Koster, R. Coehoorn, and P. A. Bobbert, Phys. Rev. Lett. **107**, 136601 (2011).

[9] M. C. J. M. Vissenberg and M. Matters, Phys. Rev. B **57**, 12964 (1998).

[10] S. D. Baranovskii, Phys. Status Solidi B **251**, 487 (2014).

[11] See Supplemental Material at http://link.aps.org/supplemental/10.1103/PhysRevB.96.241202 for discussion of the localization length, experimental methods, and description of the analytical model as well as additional experimental and analytical data including a comparison to literature data.

[12] A. Troisi and G. Orlandi, Phys. Rev. Lett. **96**, 086601 (2006).

[13] V. Rühle, A. Lukyanov, F. May, M. Schrader, T. Vehoff, J. Kirkpatrick, B. Baumeier, and D. Andrienko, J. Chem. Theory Comput. **7**, 3335 (2011).

[14] R. Volpi, S. Kottravel, M. S. Nørby, S. Stafström, and M. Linares, J. Chem. Theory Comput. **12**, 812 (2016).

[15] R. P. Fornari, P. W. M. Blom, and A. Troisi, Phys. Rev. Lett. **118**, 086601 (2017).

[16] A. Massé, P. Friederich, F. Symalla, F. Liu, V. Meded, R. Coehoorn, W. Wenzel, and P. A. Bobbert, Phys. Rev. B **95**, 115204 (2017).

[17] G. Zuo, H. Abdalla, and M. Kemerink, Phys. Rev. B **93**, 235203 (2016).

[18] G. Zuo, Z. Li, O. Andersson, H. Abdalla, E. Wang, and M. Kemerink, J. Phys. Chem. C **121**, 7767 (2017).

[19] M. Silver, L. Pautmeier, and H. Bässler, Solid State Commun. **72**, 177 (1989).

[20] V. I. Arkhipov, P. Heremans, E. V. Emelianova, and H. Bässler, Phys. Rev. B **71**, 045214 (2005).

[21] M. Lögdlund, R. Lazzaroni, S. Stafström, W. R. Salaneck, and J.-L. Brédas, Phys. Rev. Lett. **63**, 1841 (1989).

[22] R. Coehoorn, W. F. Pasveer, P. A. Bobbert, and M. A. J. Michels, Phys. Rev. B **72**, 155206 (2005).

[23] D. T. Scholes, S. A. Hawks, P. Y. Yee, H. Wu, J. R. Lindemuth, S. H. Tolbert, and B. J. Schwartz, J. Phys. Chem. Lett. **6**, 4786 (2015).

[24] N. Felekidis, A. Melianas, and M. Kemerink, Phys. Rev. B **94**, 035205 (2016).

[25] H. C. F. Martens, I. N. Hulea, I. Romijn, H. B. Brom, W. F. Pasveer, and M. A. J. Michels, Phys. Rev. B **67**, 121203 (2003).

[26] C. Tanase, P. W. M. Blom, D. M. de Leeuw, and E. J. Meijer, Phys. Status Solidi A **201**, 1236 (2004).

[27] H. van Eersel, R. A. J. Janssen, and M. Kemerink, Adv. Funct. Mater. **22**, 2700 (2012).

[28] I. A. Howard, F. Etzold, F. Laquai, and M. Kemerink, Adv. Energy Mater. **4**, 1301743 (2014).

[29] A. Melianas, F. Etzold, T. J. Savenije, F. Laquai, O. Inganäs, and M. Kemerink, Nat. Commun. **6**, 8778 (2015).

[30] K. P. Pernstich, B. Rössner, and B. Batlogg, Nat. Mater. **7**, 321 (2008).

[31] D. Venkateshvaran, M. Nikolka, A. Sadhanala, V. Lemaur, M. Zelazny, M. Kepa, M. Hurhangee, A. J. Kronemeijer, V. Pecunia, I. Nasrallah, I. Romanov, K. Broch, I. McCulloch, D. Emin, Y. Olivier, J. Cornil, D. Beljonne, and H. Sirringhaus, Nature (London) **515**, 384 (2014).

[32] Z. H. Wang, C. Li, E. M. Scherr, A. G. MacDiarmid, and A. J. Epstein, Phys. Rev. Lett. **66**, 1745 (1991).

[33] P. M. Chaikin, J. F. Kwak, and A. J. Epstein, Phys. Rev. Lett. **42**, 1178 (1979).

[34] K. van de Ruit, R. I. Cohen, D. Bollen, T. van Mol, R. Yerushalmi-Rozen, R. A. J. Janssen, and M. Kemerink, Adv. Funct. Mater. **23**, 5778 (2013).